Thermodynamics of spin-$\frac{1}{2}$ tetrameric Heisenberg antiferromagnetic chain

Shou-Shu Gong,[1] Song Gao,[2] and Gang Su[1,*]

[1]*College of Physical Sciences, Graduate University of Chinese Academy of Sciences, P.O. Box 4588, Beijing 100049, People's Republic of China*

[2]*College of Chemistry and Molecular Engineering, State Key Laboratory of Rare Earth Materials Chemistry and Applications, Peking University, Beijing 100871, People's Republic of China*

(Received 9 January 2009; revised manuscript received 7 May 2009; published 10 July 2009)

The thermodynamic properties of a spin $S=1/2$ tetrameric Heisenberg antiferromagnetic chain with alternating interactions AF_1-AF_2-AF_1-F (AF and F denote the antiferromagnetic and ferromagnetic couplings, respectively) are studied by means of the transfer-matrix renormalization-group method and Jordan-Wigner transformation. It is found that in the absence of magnetic field, the thermodynamic behaviors are closely related to the gapped low-lying excitations, and a novel structure with three peaks in the temperature dependence of specific heat is unveiled. In a magnetic field, a phase diagram in the temperature-field plane for the couplings satisfying $J_{AF_1}=J_{AF_2}=J_F$ is obtained, in which various phases are identified. The temperature dependence of thermodynamic quantities including the magnetization, susceptibility, and specific heat are studied to characterize the corresponding phases. It is disclosed that the magnetization has a crossover behavior at low temperature in the Luttinger liquid phase, which is shown falling into the same class as that in the $S=1$ Haldane chain. In the plateau regime, the thermodynamic behaviors alter at a certain field, which results from the crossing of two excitation spectra. By means of the fermion mapping, it is uncovered that the system has four spectra from fermion and hole excitations that are responsible for the observed thermodynamic behaviors.

DOI: 10.1103/PhysRevB.80.014413 PACS number(s): 75.10.Jm, 75.40.Cx, 75.40.Mg

I. INTRODUCTION

In recent years, low-dimensional quantum magnets have received much attention in condensed-matter physics. In particular, one-dimensional quantum spin chains with competing interactions that show exotic physical properties have been extensively studied in the past decades. Among others, the dimerized spin-$\frac{1}{2}$ antiferromagnetic (AF)-ferromagnetic (F) alternating chain has been widely studied both theoretically[1–3] and experimentally,[4] where it was found that the system has a gap from the singlet ground state to the triplet excited states, and can be mapped onto the $S=1$ Haldane chain[5–7] if the F couplings dominate. Moreover, a series of trimerized compounds, including the $S=1/2$ antiferromagnetic F-F-AF chain of $3CuCl_2\cdot 2dx$ (dx=1,4-dioxane) (Ref. 8) and the ferrimagnetic AF-AF-F chains of $[Mn(L_2)(N3)_2]_n$ (L=3-methylpyridine) with $S=5/2$,[9] $[M(4,4'bipy)(N_3)_2]_n$ (bipy=bipyridine) with M=Co ($S=3/2$) and Ni ($S=1$),[10] and $[Mn(N_3)_2(bpee)]_n$ [bpee=trans-1,2-bis(4-pyridyl)ethylene] with $S=5/2$,[11] have been synthesized in experiments. In such trimerized spin chains, the topological quantization of magnetization, i.e., the magnetization plateau, has been predicted theoretically.[12–16] The predictions were based on the theorem proposed by Oshikawa, Yamanaka, and Affleck,[17] which extends the Lieb-Schultz-Mattis theorem to give a necessary condition for the appearance of magnetization plateau in the spin chains with translational symmetry. However, the plateau was not observed experimentally in the above-mentioned compounds owing to the weak AF couplings. A plateau at $m=1/4$ (m is the magnetization per site) was later observed in an $S=1/2$ tetrameric F-F-AF-AF ferrimagnet $Cu(3\text{-}Clpy)_2(N_3)_2$ (Refs. 18–22) due to the strong AF couplings.

Recently, a spin $S=1/2$ tetrameric Heisenberg antiferromagnetic chain (HAFC) with AF_1-AF_2-AF_1-F interactions has been studied, whose ground state was found to be in a gapped Haldane-type phase while, importantly, it cannot be reduced to an integer spin chain.[23] 26 years ago, Haldane[24] conjectured that an isotropic HAFC with an integer spin has a finite gap from the singlet ground state to the triplet excited states and the spin-spin correlation function decays exponentially, while the HAFC with half-integer spin has a gapless spectrum and a correlation function with a power-law decay. Although there is no rigorous proof for a general case until now, Haldane's scenario has been confirmed experimentally and numerically in many systems (e.g., Ref. 25). Besides the HAFCs with integer spin, Haldane gap has also been found in $S=1/2$ spin ladders[26,27] and AF-F alternating Heisenberg chains.[5] This is because these spin-$\frac{1}{2}$ systems were found to be reducible to an $S=1$ HAFC when the F couplings are dominantly larger than the AF couplings. However, the present $S=1/2$ AF_1-AF_2-AF_1-F tetrameric HAFC cannot be reduced to an integer spin chain even if the F coupling dominates and a gapped state with $m=0$ was observed.[23] By using a dual transformation, the $Z_2\times Z_2$ hidden symmetry is disclosed to be fully broken and the string order is found nonvanishing in the ground state further suggesting that this spin-$\frac{1}{2}$ tetrameric HAFC system belongs to the Haldane-type phase,[28,29] which extends the substance of Haldane's scenario, namely, the Haldane gap can appear in certain spin half-integer chains. Apart from the gapped state with $m=0$, a magnetization plateau at $m=1/4$ was also found in this system.[23] In the critical magnetic fields where the magnetization curve is singular, quantum phase transitions (QPTs) (Ref. 30) may happen and consequently, phase crossovers are expected at finite temperature.

As this spin-$\frac{1}{2}$ AF_1-AF_2-AF_1-F tetrameric HAFC exhibits many interesting behaviors at zero temperature, a deeper in-

vestigation is still quite necessary. In this paper, we shall go on elaborating the thermodynamics of this system by means of the transfer-matrix renormalization group (TMRG) as well as the Jordan-Wigner (JW) transformation with emphasis on the effects of the couplings and the external magnetic field on thermodynamical properties of the system. The possible magnetic phase diagram at finite temperature will be presented. The low-lying excitations that are closely related to the observed thermodynamic behaviors will also be discussed.

The Hamiltonian of the $S=1/2$ tetrameric HAFC with alternating couplings AF_1-AF_2-AF_1-F in a longitudinal magnetic field is given by

$$H=\sum_{j=1}^{N}(J_{AF_1}\mathbf{S}_{4j-3}\cdot\mathbf{S}_{4j-2}+J_{AF_2}\mathbf{S}_{4j-2}\cdot\mathbf{S}_{4j-1}+J_{AF_1}\mathbf{S}_{4j-1}\cdot\mathbf{S}_{4j}-J_F\mathbf{S}_{4j}\cdot\mathbf{S}_{4j+1})-h\sum_{j=1}^{4N}S_j^z, \quad (1)$$

where $J_{AF_{1,2}}(>0)$ denote the AF couplings, $J_F(>0)$ denotes the F coupling, and h is the magnetic field. We take J_{AF_1} as the energy scale and $g\mu_B=1$ for convenience. N is the total number of the unit cells. The Boltzmann constant is taken as $k_B=1$.

The numerical algorithm TMRG method,[31–34] which is a powerful tool for studying the thermodynamics of one-dimensional quantum systems will be primarily employed in the following investigations. As the TMRG technique has been discussed in many reviews, we shall not repeat the details here. In the following calculations, the width of the imaginary time slice is taken as $\varepsilon=0.1$ and the error caused by the Trotter-Suzuki decomposition is less than 10^{-3}. During the TMRG iterations, 80 states are retained and the temperature is down to $T=0.02J_{AF_1}$ in general. In the Luttinger liquid and gapless phases, the temperature is down lower than $0.01J_{AF_1}$ when calculating the magnetization and susceptibility. The truncation error is less than 10^{-4} in all calculations.

The other parts of the paper are organized as follows. In Sec. II, we shall present the TMRG results of the thermodynamic quantities in the absence of magnetic field. In Sec. III, a magnetic phase diagram at finite temperature will be proposed for the case with $J_{AF_1}=J_{AF_2}=J_F$ and the thermodynamic properties will be discussed in the various phases. In Sec. IV, we shall invoke the mean-field results from the JW transformation to explain the behaviors observed in Secs. II and III. Finally, a summary and discussion will be given.

II. ZERO-FIELD THERMODYNAMIC PROPERTIES

A. Specific heat

Let us first look at the temperature dependence of the specific heat for the isolated tetramer systems with $J_{AF_2}=0$ or $J_F=0$. For $J_{AF_2}=0$, the specific heat decays exponentially as $T\to 0$ and has a sharp peak at low temperature that shifts slightly to lower temperatures with increasing J_F, as shown in Fig. 1(a). For $J_F=0$, the specific heat has a single peak

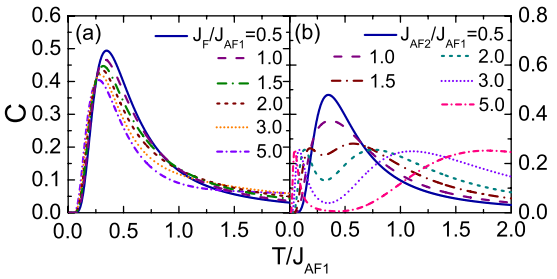

FIG. 1. (Color online) Temperature dependence of the specific heat of the isolated tetramer systems with (a) $J_{AF_2}=0$ and (b) $J_F=0$.

when $J_{AF_2}/J_{AF_1}<1$. If J_{AF_2} exceeds J_{AF_1}, with increasing J_{AF_2} the single peak splits into double peaks, one of which moves to lower temperatures while the other moves to higher temperatures, as shown in Fig. 1(b). The distinct behaviors of the specific heat for the two tetramer systems are owing to their different energy spectra. When $J_{AF_2}=0$, for each tetramer there are four energy levels that decrease with increasing J_F, while the gaps among them vary slightly, yielding a small shift of the peak. When $J_F=0$, with increasing J_{AF_2} the gap between the ground state and the first excited states diminishes rapidly, accounting for the shift of the low-temperature peak, while the shift of the high-temperature peak is owing to the enlarged gaps between the energy levels. These limiting cases offer useful information for better understanding the features of the specific heat of the systems with arbitrary couplings, which will be discussed below.

The effects of J_F on the specific heat are first discussed. In Fig. 2(a), the specific heat of the system with $J_{AF_2}/J_{AF_1}=1.0$ are presented for different J_F. The specific heat has a single peak and decays exponentially as $T\to 0$, indicating a gapped excitation. With increasing J_F, the single peak declines and a shoulder appears to be gradually promi-

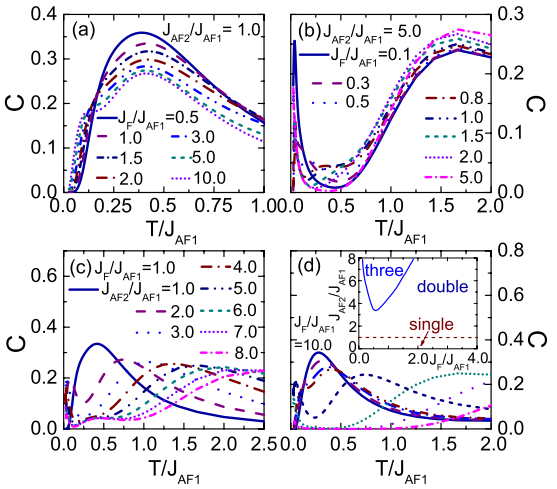

FIG. 2. (Color online) Temperature dependence of the specific heat of the tetrameric chain for (a) $J_{AF_2}/J_{AF_1}=1.0$, (b) $J_{AF_2}/J_{AF_1}=5.0$, (c) $J_F/J_{AF_1}=1.0$, and (d) $J_F/J_{AF_1}=10.0$ with $J_{AF_2}/J_{AF_1}=0.5$, 0.7, 0.9, 1.0, 2.0, 5.0, 8.0, and 12.0 from top to bottom. The inset of (d) shows the parameter regions where the specific heat has different peak structures.

nent at low temperatures. Thus, it is expected that the system has at least two gapped excitations. With increasing J_F, the gap that is related to the lower excitation decreases slowly,[23] yielding the emergence of the shoulder. Figure 2(b) shows the specific heat of the system with $J_{AF_2}/J_{AF_1}=5.0$ for different J_F. As J_{AF_2} is large, the specific heat has two peaks for $J_F/J_{AF_1}=0.1$, like the tetramer system with $J_F=0$. With increasing J_F, a novel peak emerges between the low- and high-temperature peaks, which shifts to higher temperatures with further increase in the F coupling until it is merged into the high-temperature peak. It can be seen that the specific heat behaves rather differently with J_F for different J_{AF_2} and in certain couplings region the specific heat can exhibit a novel three-peak structure.

Next, we study the effects of J_{AF_2} on the specific heat. In Fig. 2(c), the specific heat of the system with $J_F/J_{AF_1}=1.0$ are plotted for various J_{AF_2}. When $J_{AF_2}=J_{AF_1}$, the specific heat has a single peak and decays exponentially as $T\to 0$. When J_{AF_2} exceeds J_{AF_1}, the single peak splits into double peaks, one of which shifts to lower temperature side while another moves to the higher temperature side with increasing J_{AF_2}. These behaviors could be understood by means of the corresponding tetramer system where the gaps between the energy levels are decreasing rapidly with increasing J_{AF_2}.[23] It is noticed that the novel peak emerges when J_{AF_2} is large enough, e.g., $J_{AF_2}/J_{AF_1}=4.0$ for $J_F/J_{AF_1}=1.0$. When J_{AF_2} continues to increase, the novel peak is nearly invariant. When J_F is too large, as shown in Fig. 2(d) for $J_F/J_{AF_1}=10.0$, the novel peak is absent. These results indicate that the novel peak is yielded by increasing J_F after the double peaks have been induced by large J_{AF_2}.

The inset of Fig. 2(d) shows the parameter regions where the specific heat has different peak structures. The dashed line separates the regions of the single peak and double peaks while the solid line separates the regions of the double and three peaks. The observations in Figs. 2(a)–2(c) are manifested clearly in this depiction. It is shown that when $J_{AF_2}>J_{AF_1}$, the single peak starts to split into double peaks. When J_{AF_2}/J_{AF_1} exceeds about 3.5, the novel peak can appear with increasing J_F, and it would merge into the high-temperature peak with further increase in the coupling. As the intermediate region is enlarged by increasing J_{AF_2}, the parameter region of J_F for the emergence of the novel peak is wider for larger J_{AF_2}. It is interesting to point out that the emergence of three peaks of the specific heat in the absence of magnetic field is nontrivial, which is not the usual feature in low-dimensional quantum magnets.

B. Susceptibility

The temperature dependence of the susceptibility is presented in Fig. 3 for different cases. It is shown that the susceptibility has a peak and decreases exponentially as $T\to 0$. With increasing J_F or J_{AF_2}, the peak shifts to lower temperatures with the height enhanced, which are consistent with the diminution of the gap and the behaviors of the specific heat. As the gap decreases slowly with J_F but rapidly with J_{AF_2},[23] the susceptibility changes slightly with J_F but dramatically

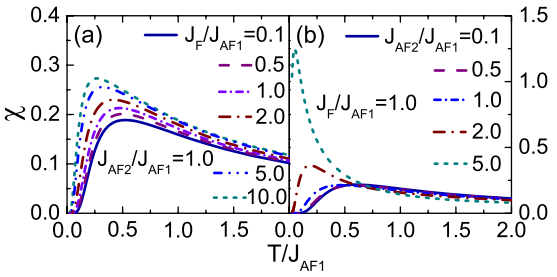

FIG. 3. (Color online) Temperature dependence of the spin susceptibility of the tetrameric chain for (a) $J_{AF_2}/J_{AF_1}=1.0$ with different J_F and (b) $J_F/J_{AF_1}=1.0$ with different J_{AF_2}.

with J_{AF_2}, as demonstrated in Figs. 3(a) and 3(b), respectively. At high temperatures, the gap is suppressed by thermal fluctuations and the susceptibility goes to coincidence for different couplings. These behaviors imply the distinctions of the low-lying excitations, which will be reexamined in terms of the spinless fermions in Sec. IV.

III. THERMODYNAMICS IN MAGNETIC FIELDS

In this section, the thermodynamic properties of the system with $J_{AF_1}=J_{AF_2}=J_F$ in the presence of a magnetic field are studied by means of the TMRG method. A phase diagram in the temperature-field plane is proposed and the magnetization, susceptibility, and specific heat are investigated accordingly in the various phases.

A. Phase diagram

As shown in Fig. 4(a), the zero-temperature magnetization curve is singular at the critical fields h_{c_1}, h_{c_2}, h_{c_3}, and h_s,[23] suggesting that QPTs (Ref. 30) may happen. These transitions are measured by the divergent peaks of $\partial m/\partial h$, which separate the Haldane-type phase, Luttinger liquid (LL) phase, plateau phase, gapless phase, and polarized state of the system in a magnetic field. At finite temperature, the magnetization plateaus are smeared out, and the peaks of $\partial m/\partial h$ become analytic, which, however, can still describe the crossover behaviors of the various phases. Therefore, the magnetization process at different temperatures will be studied to obtain the phase diagram in the temperature-field plane.

Figure 4(a) shows that with increasing temperature, the two peaks of $\partial m/\partial h$ at $h_{c_1}(h_{c_3})$ and $h_{c_2}(h_s)$ gradually merge into a single peak at rather low temperature, indicating the crossovers from the LL (gapless) regime to other regimes. With further increasing temperature, the high-field peak that separates the plateau and spin-polarized regimes disappears at $T\approx 0.44J_{AF_1}$ and the low-field peak that separates the gapped spin liquid and plateau regimes disappears at $T\approx 0.68J_{AF_1}$ [the inset of Fig. 4(a)]. The shifts of the peaks in the temperature-field plane compose of the crossover lines. Based on the observations, we propose a phase diagram in the temperature-field plane as shown in Fig. 4(b), from which one may observe that the system has the gapped

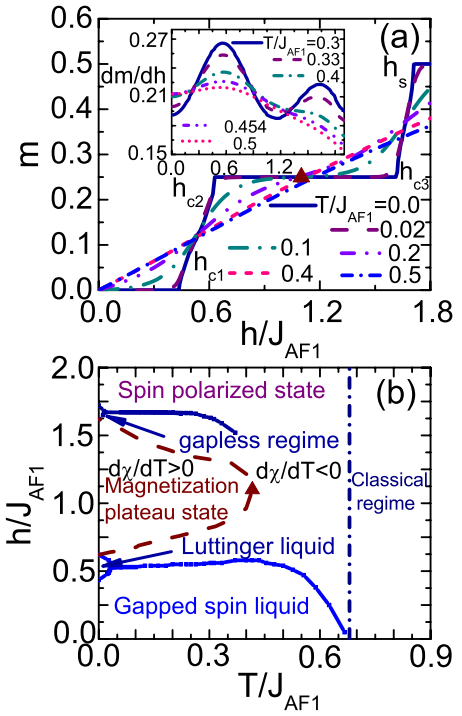

FIG. 4. (Color online) (a) Magnetization curves at different temperatures. The inset shows $\partial m/\partial h$ as a function of h at different temperatures. (b) Phase diagram in the temperature-field plane. The solid lines and the dashed line are obtained by observing the peaks of $\partial m/\partial h$ and the points with $\partial\chi/\partial T=0$, respectively.

spin liquid, LL, magnetization plateau, gapless, spin polarized, and classical phases.

B. Magnetization

The temperature dependence of the magnetization $m(T)$ in the various regimes are investigated. When $h<h_{c_1}$, the low-lying excitation is gapped. With decreasing temperature, the magnetization m first increases with a power law, then goes down, and finally decays exponentially to zero with the effective gap $\Delta_{\text{eff}}=h_{c_1}-h$ as $T\to 0$. As expected, with decreasing the effective gap, the peak of $m(T)$ moves to lower temperature side with the amplitude enhanced, as shown in Fig. 5(a).

In the LL regime when $h_{c_1}<h<h_{c_2}$, the gap is closed by the field, and the system undergoes a commensurate-incommensurate transition at $h=h_{c_1}$ in the ground state.[35] At finite temperatures, $m(T)$ shows a minimum or maximum at low temperatures, as shown in Fig. 5(b). The minima are close to the crossover boundary between the gapped spin liquid and LL regimes while the maxima are close to that between the magnetization plateau and LL regimes, indicating the nonsingular crossovers from the LL to the high-temperature regimes. Maeda, Hotta, and Oshikawa[36] pointed out that this crossover is universal in general gapped one-dimensional spin systems with axial symmetry, resulting from the minus derivative of the density of states near the critical field and the variation of the Fermi velocity v_F. In Sec. IV, this observation would be reproduced by the JW

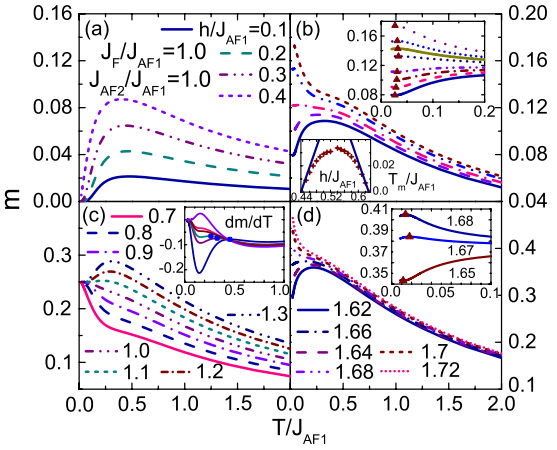

FIG. 5. (Color online) Magnetization as a function of temperature for (a) $h<h_{c_1}$, (b) $h_{c_1}<h<h_{c_2}$, (c) $h_{c_2}<h<h_{c_3}$, and (d) $h_{c_3}<h<h_s$. The insets show (b) the minima (maxima) and the field dependence of the crossover temperature; (c) the behavior of $\partial m/\partial T$ for $h/J_{\text{AF}_1}=0.9$, 1.0, 1.02, 1.04, 1.05, and 1.1 from bottom to top; and (d) the minima and maxima in the gapless regime.

transformation and interpreted more physically.

In Ref. 36, a linear dependence of the transition temperature (T_m) on the field $T_m=x_0(h-h_c)$ (h_c is the critical field where the gap is closed) near the critical field h_c was proposed for the $S=1$ Haldane chain. The field dependence of the crossover temperature for the present tetrameric HAFC is shown in the lower inset of Fig. 5(b). It can be seen that the crossover temperature T_m varies like a sine function of the field and behaves linearly near the critical fields h_{c_1} and h_{c_2}. The coefficient $x_0\simeq 0.762\,38$ proposed in Ref. 36 for the $S=1$ Haldane chain near h_c fits well to our data near both h_{c_1} and h_{c_2} (see the solid lines in the inset), indicating that this tetrameric chain slightly above h_{c_1} and below h_{c_2} could also be well described by the free fermion theory,[37–39] and the crossover in this LL phase is of the same class as that in the Haldane chain. Although this tetrameric chain cannot be reduced to a typical Haldane chain with an integer spin, their analogous dispersion relation of the low-lying excitations are revealed by the same class of this crossover behavior of magnetization.

In the magnetization plateau, m approaches 0.25 as $T\to 0$. As shown in Fig. 5(c), when $h_{c_2}<h<h_m\simeq 1.1J_{\text{AF}_1}$, m increases slowly with cooling temperature to a certain value and, then, rises rapidly to 0.25, where h_m is the crossing field of the magnetization curves at low temperatures in the plateau states, as marked by the triangle in Fig. 4(a). When $h_m<h<h_{c_3}$, m increases to a maximum and then declines to 0.25. The different behaviors are also observed in the magnetization curves at various temperatures [Fig. 4(a)]. In the field h_m, m changes slowly at low temperature, like the $m(T)$ curve with $h/J_{\text{AF}_1}=1.1$ in Fig. 5(c). These magnetic behaviors in the plateau state have also been noted in the spin-$\frac{1}{2}$ trimerized[15] and F-F-AF-AF tetrameric chains.[19] In Sec. IV, it would be found that these common features in the plateau states may result from the crossing of fermion and hole excitations. The field h_m is in the middle of the plateau and corresponds to the midpoint of the gap between the crossing

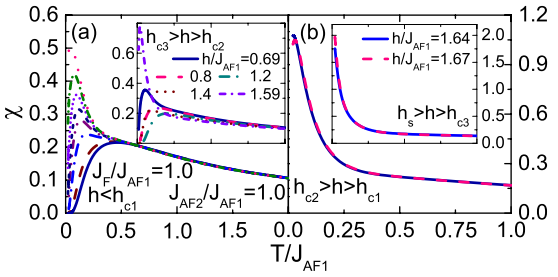

FIG. 6. (Color online) Temperature dependence of the susceptibility for (a) h/J_{AF_1}=0.1, 0.2, 0.3, 0.34, 0.36, 0.38, 0.4, and 0.42 from bottom to top; (b) h/J_{AF_1}=0.5 and 0.55; the inset of (a) $h_{c_3}>h>h_{c_2}$ and (b) $h_s>h>h_{c_3}$.

fermion and hole spectra. When $h>h_m$, the maximum of $m(T)$ with $\partial m/\partial T=0$ measures the change in the magnetic properties. For $h<h_m$, although m keeps declining, such a change also exists, which can be visible in the temperature dependence of $\partial m/\partial T$. Corresponding to $\partial m/\partial T=0$ for $h>h_m$, $\partial m/\partial T$ has maxima that are marked by solid squares to separate the high-temperature regime for $h<h_m$, as shown in the inset of Fig. 5(c). As the field approaches h_m, the maximum tends to disappear.

In the gapless regime, the gap in the plateau state can be closed by increasing the field. Thus, the magnetic behavior $m(T)$ is analogous to that in the LL phase, where there are also minimum and maximum observed at rather low temperatures [Fig. 5(d)]. Such a crossover in the gapless phase between a $m\neq 0$ plateau and the saturated state has not been reported. The magnetic behaviors of the spin-$\frac{1}{2}$ F-F-AF antiferromagnetic chain[15] have been studied numerically but no such a crossover is observed between the $m=1/6$ plateau and the saturated state when the temperature is down to $0.025J_{\mathrm{F}}$. It is also noticed that the crossover temperatures in the gapless regime are lower than those in the LL phase, which would be interpreted in terms of the spinless fermion in Sec. IV.

C. Susceptibility

The behaviors of the susceptibility χ in the various regimes will be discussed in this subsection. When h/J_{AF_1} is less than about 0.3 in the gapped spin liquid, χ has a single peak at $T\simeq\Delta$ (Δ is the gap in the absence of magnetic field), and approaches zero exponentially as $T\to 0$. With further increasing h, a new peak emerges and moves to lower temperatures with the height enhanced while the high-temperature peak becomes smoother, as shown in Fig. 6(a). In the high-temperature region $T>\Delta$, the susceptibility under different fields coincide because the gap is suppressed by thermal fluctuations. In the fermion mapping in Sec. IV, the system has two positive-energy excitations (fermion excitations) and two minus energy excitations (hole excitations) when $h=0$. With the decrease in the excitation energies induced by increasing the field, the susceptibility contributed from the fermion excitations moves to lower temperatures with the amplitude enhanced while that from the hole excitations shifts to higher temperatures with the height decreased, both of which are responsible for the behaviors observed in Fig. 6(a). In the LL, χ is finite as $T\to 0$, as shown in Fig. 6(b). With cooling temperature, χ increases slowly to the temperature $T\simeq\Delta$ and then has a sharp rise until to a peak at rather low temperatures, which results from the closure of the gap.

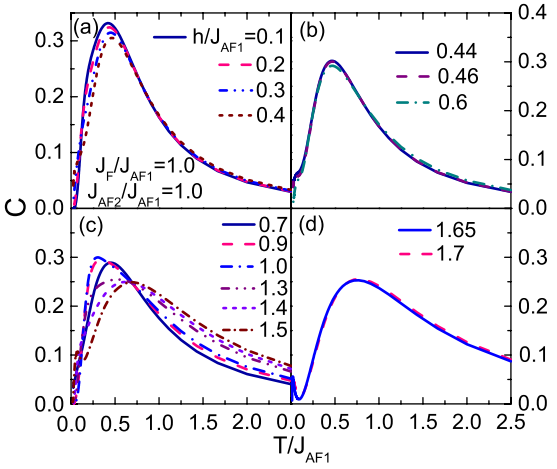

FIG. 7. (Color online) Specific heat of the system with (a) $h_{c_1}>h$, (b) $h_{c2}>h>h_{c1}$, (c) $h_{c3}>h>h_{c2}$, and (d) $h_s>h>h_{c3}$.

In the plateau state, due to the open of a gap, the susceptibility has a single peak, and approaches zero exponentially as $T\to 0$. With increasing the field, the peak moves to higher temperatures with the height declined when $h<h_m$ while it shifts to lower temperatures with the height enhanced after h exceeds h_m, as shown in the inset of Fig. 6(a). The field dependence of the peak temperature is displayed by the dashed line in Fig. 4(b), where the field with the highest peak temperature is h_s, as marked by a triangle. These distinct behaviors of the susceptibility also result from the crossing of the fermion and hole spectra. When $h<h_m$, χ is dominated by a hole branch whose gap is enhanced with increasing the field, yielding the peak to move to higher temperatures with the height decreased. After h exceeds h_m, the two spectra cross and the susceptibility is dominated by the fermion branch whose gap declines with the increasing field, yielding the peak to move to lower temperatures with the height enhanced. Different from the gapped spin liquid, the susceptibility does not show double peaks in the plateau phase. In the gapless regime, owing to the closure of the gap, the susceptibility exhibits the same features as those in the LL, as shown in the inset of Fig. 6(b).

D. Specific heat

In this subsection, the specific heat is explored in detail. When $h<h_{c_1}$, the specific heat C has a single peak and approaches zero exponentially as $T\to 0$. The peak shifts to higher temperatures with the height decreased when Δ_{eff} diminishes [Fig. 7(a)]. This shift is attributed to the hole excitations whose gaps increase with increasing the field. It is noticed that the peak temperature, $T_{\mathrm{peak}}/J_{\mathrm{AF}_1}\simeq\Delta$, in this system is distinct from the result $T_{\mathrm{peak}}/J\simeq 2\Delta'$ of the $S=1$ Haldane chain (J and Δ' are the coupling and gap of the

$S=1$ Haldane chain, respectively).[40] As the field h approaches h_{c_1}, a shoulder gradually emerges at low temperature, which is a signature of approaching the quantum critical point[30,41] and is from the hole excitations.

In the LL, the linear temperature dependence of the specific heat at low temperature is observed. With a further increase in the field, the system shifts away from the quantum critical point h_{c_1}. Thus, the shoulder at low temperature is smoothed down gradually, as shown in Fig. 7(b). The disappearance of the shoulder is attributed to the hole excitations.

In the plateau state, the specific heat decays exponentially when $T\rightarrow 0$ because of the open of a gap. Near the lower critical field h_{c_2}, the shoulder that emerges in the LL vanishes gradually while near the upper critical field h_{c_3}, a double-peak structure emerges. As expected, the crossing of the fermion and hole spectra affects the behavior of the specific heat. With increasing the field, the peak of the specific heat moves to lower temperatures when $h<h_m$, and when h exceeds h_m, the peak starts to move to higher temperatures, as shown in Fig. 7(c). However, different from the magnetization and susceptibility, the behavior of the specific heat cannot be characterized simply only by the hole $(h<h_m)$ or fermion $(h>h_m)$ excitations, although the crossing indeed changes the features of the behavior. This is because the magnetization and susceptibility are determined only by the occupied number of the excitations but the specific heat is affected by both the numbers and energies of the quasiparticles.

In the gapless regime, with increasing the field, the high-temperature peak of the specific heat keeps nearly intact while the low-temperature peak that occurs near the critical field h_{c_3} in the plateau state moves to lower temperatures with the height declined [Fig. 7(d)]. These behaviors will be analyzed in the next section.

IV. JORDAN-WIGNER TRANSFORMATION AND SPINLESS FERMION MAPPING

In order to explain the thermodynamic behaviors observed in the above sections, the elementary excitations of the system are studied using the JW transformation.[42] The $S=1/2$ spin operators can be transformed into the spinless fermion operators through JW transformation

$$S_i^+ = c_i^\dagger e^{i\pi\Sigma_{j<i}c_j^\dagger c_j}, \quad S_i^z = \left(c_i^\dagger c_i - \frac{1}{2}\right), \tag{2}$$

where $c_i^\dagger$ and c_i are the creation and annihilation operators of the spinless fermion, respectively. For this $S=1/2$ tetrameric HAFC, four kinds of spinless fermions should be introduced:

$$S_{4j-3}^+ = a_j^\dagger \exp\left[i\pi\sum_{m<j}(a_m^\dagger a_m + b_m^\dagger b_m + c_m^\dagger c_m + d_m^\dagger d_m)\right],$$

$$S_{4j-2}^+ = b_j^\dagger \exp\left\{i\pi\left[\sum_{m<j}(a_m^\dagger a_m + b_m^\dagger b_m + c_m^\dagger c_m + d_m^\dagger d_m) + a_j^\dagger a_j\right]\right\},$$

$$S_{4j-1}^+ = c_j^\dagger \exp\left\{i\pi\left[\sum_{m<j}(a_m^\dagger a_m + b_m^\dagger b_m + c_m^\dagger c_m + d_m^\dagger d_m) + a_j^\dagger a_j + b_j^\dagger b_j\right]\right\},$$

$$S_{4j}^+ = d_j^\dagger \exp\left\{i\pi\left[\sum_{m<j}(a_m^\dagger a_m + b_m^\dagger b_m + c_m^\dagger c_m + d_m^\dagger d_m) + a_j^\dagger a_j + b_j^\dagger b_j + c_j^\dagger c_j\right]\right\},$$

$$S_{4j-3}^z = a_j^\dagger a_j - \frac{1}{2}, \quad S_{4j-2}^z = b_j^\dagger b_j - \frac{1}{2},$$

$$S_{4j-1}^z = c_j^\dagger c_j - \frac{1}{2}, \quad S_{4j}^z = d_j^\dagger d_j - \frac{1}{2}. \tag{3}$$

After making the JW transformation, the XY interactions of original Hamiltonian are transformed to the nearest-neighbor hoppings of the fermions and the Ising terms become the nearest-neighbor density-density interactions that will be treated by the Hartree-Fock (HF) approximation. By performing a cumbersome derivation, we obtain a mean-field Hamiltonian after omitting the constant

$$H_{\mathrm{HF}}=\sum_{j=1}^{N}\left\{\frac{1}{2}\left[J_{\mathrm{AF}_1}\left(d_b-\frac{1}{2}\right)-J_{\mathrm{F}}\left(d_d-\frac{1}{2}\right)\right]a_j^{\dagger}a_j+\frac{1}{2}\left[J_{\mathrm{AF}_1}\left(d_a-\frac{1}{2}\right)+J_{\mathrm{AF}_2}\left(d_c-\frac{1}{2}\right)\right]b_j^{\dagger}b_j\right.$$
$$+\frac{1}{2}\left[J_{\mathrm{AF}_2}\left(d_b-\frac{1}{2}\right)+J_{\mathrm{AF}_1}\left(d_d-\frac{1}{2}\right)\right]c_j^{\dagger}c_j+\frac{1}{2}\left[J_{\mathrm{AF}_1}\left(d_c-\frac{1}{2}\right)-J_{\mathrm{F}}\left(d_a-\frac{1}{2}\right)\right]d_j^{\dagger}d_j+J_{\mathrm{AF}_1}\left(\frac{1}{2}-p_{AB}\right)a_j^{\dagger}b_j$$
$$\left.+J_{\mathrm{AF}_2}\left(\frac{1}{2}-p_{BC}\right)b_j^{\dagger}c_j+J_{\mathrm{AF}_1}\left(\frac{1}{2}-p_{CD}\right)c_j^{\dagger}d_j-J_{\mathrm{F}}\left(\frac{1}{2}-p_{DA}\right)d_j^{\dagger}a_{j+1}+\mathrm{h.c.}\right\}-h\sum_{j=1}^{N}(a_j^{\dagger}a_j+b_j^{\dagger}b_j+c_j^{\dagger}c_j+d_j^{\dagger}d_j),\qquad(4)$$

where the occupied fermion numbers are $d_a=\langle a_j^{\dagger}a_j\rangle$, $d_b=\langle b_j^{\dagger}b_j\rangle$, $d_c=\langle c_j^{\dagger}c_j\rangle$, and $d_d=\langle d_j^{\dagger}d_j\rangle$, and the covalent bondings are $p_{AB}=\langle b_j^{\dagger}a_j\rangle$, $p_{BC}=\langle c_j^{\dagger}b_j\rangle$, $p_{CD}=\langle d_j^{\dagger}c_j\rangle$, and $p_{DA}=\langle a_{j+1}^{\dagger}d_j\rangle$. The brackets $\langle\cdots\rangle$ denote either the HF ground-state average ($T=0$) or the thermal average ($T\neq 0$). By making the Fourier transform and then Bogoliubov transformations, a quadratic Hamiltonian can be obtained

$$H_{\mathrm{HF}}=\sum_{k}(\omega_k^{\alpha}\alpha_k^{\dagger}\alpha_k+\omega_k^{\beta}\beta_k^{\dagger}\beta_k+\omega_k^{\gamma}\gamma_k^{\dagger}\gamma_k+\omega_k^{\lambda}\lambda_k^{\dagger}\lambda_k),\qquad(5)$$

where α, β, γ, and λ denote four excitation spectra with the dispersion relations ω_k^i $(i=\alpha,\beta,\gamma,\lambda)$.

A. Spin gap and magnetization

In the mean-field calculations of the ground-state properties, the occupation numbers and covalent bondings are self-consistently calculated by minimizing the ground-state energy with the constraint $\langle S_{\mathrm{tot}}^z\rangle=\langle\Sigma_{i=1}^{4N}S_i^z\rangle=0$, i.e., the total number of spinless fermions is $2N$. The self-consistent calculations give rise to four excitation spectra [Fig. 8(a)]. In the absence of magnetic field, $\omega_k^{\alpha}=-\omega_k^{\lambda}$ and $\omega_k^{\beta}=-\omega_k^{\gamma}$. Thus, the ground state is obtained by filling up the two negative spectra α and β. The gap from $S_{\mathrm{tot}}^z=0$ to $S_{\mathrm{tot}}^z=\pm 1$, corresponds to the energy of adding or removing a fermion

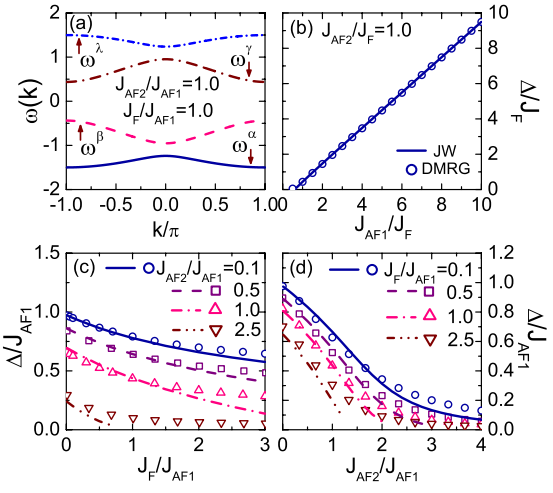

FIG. 8. (Color online) (a) The elementary excitation spectra of the system. The gap as a function of (b) J_{AF_1}, (c) J_{F}, and (d) J_{AF_2}. The DMRG results are from Ref. 23.

$$\Delta_{\mathrm{HF}}=\omega_{k=\pi}^{\gamma}$$
$$=\frac{\sqrt{2}}{4}\{A-\{A^2-4[J_{\mathrm{AF}_1}^4(1+2p_{AB})^2\times(1+2p_{CD}^2)-2J_{\mathrm{AF}_1}^2J_{\mathrm{AF}_2}J_{\mathrm{F}}(1+2p_{AB})\times(1+2p_{BC})(1+2p_{CD})(1+2p_{DA})+J_{\mathrm{AF}_2}^2J_{\mathrm{F}}^2(1+2p_{BC})^2(1+2p_{DA})^2]\}^{1/2}\}^{1/2},\qquad(6)$$

where the parameter A is

$$A=J_{\mathrm{AF}_1}^2[(1+2p_{AB})^2+(1+2p_{CD})^2]+J_{\mathrm{AF}_2}^2(1+2p_{BC})^2+J_{\mathrm{F}}^2(1+2p_{DA})^2.\qquad(7)$$

For $J_{\mathrm{AF}_1}=J_{\mathrm{AF}_2}=J_{\mathrm{F}}=1$, the mean-field result gives the gap $\Delta_{\mathrm{HF}}=0.4377J_{\mathrm{AF}_1}$, which agrees with the DMRG result $\Delta=0.435J_{\mathrm{AF}_1}$.[23]

In Fig. 8(b), the gap is plotted as a function of J_{AF_1}. The HF results agree with the DMRG values when $J_{\mathrm{AF}_1}/J_{\mathrm{F}}>0.7$. In Figs. 8(c) and 8(d), J_{F} and J_{AF_2} dependences of the gap are plotted, respectively. It can be seen that when J_{F} and J_{AF_2} are smaller than J_{AF_1}, the HF results are consistent with the DMRG results but with increasing J_{F} or J_{AF_2}, the HF results become worse when J_{F} or J_{AF_2} is prominent.

In a magnetic field, new quasiparticles can be excited in the γ and λ branches. It is found that the excited fermions can interpret the magnetization process at zero temperature. When the field is less than the gap, no fermion is excited and $m=0$. When the field closes the gap at h_{c_1}, new fermions are excited in the γ branch, and m increases until the γ branch is fully filled at h_{c_2}. The gap between the spectra γ and λ is the width of the plateau, say, $h_{c_3}-h_{c_2}$. When the field exceeds h_{c_3}, the fermions in the spectrum λ are excited and the system is fully spin polarized.

B. Zero-field thermodynamics

At finite temperature, the numbers of the excitations obey the Fermi-distribution function $n_k^i=1/(e^{\omega_k^i/T}+1)$ $(i=\alpha,\beta,\gamma,\lambda)$, from which the thermodynamics can be obtained by the self-consistent calculations for the occupation numbers and covalent bondings.

In Fig. 9, the specific heat obtained from the HF calculations are displayed, which qualitatively agree with the

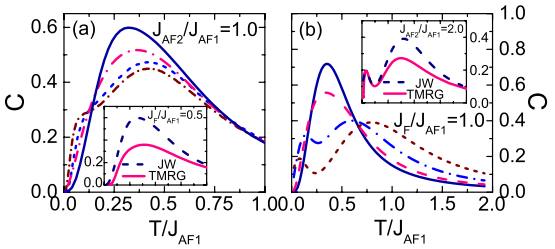

FIG. 9. (Color online) Temperature dependence of the specific heat for (a) J_F/J_{AF_1}=0.5, 1.5, 2.5, and 3.0; and (b) J_{AF_2}/J_{AF_1}=0.5, 1.0, 1.5 and 2.0 from top to bottom. The comparisons with the TMRG results are shown in the insets.

TMRG results. With increasing J_F or J_{AF_2}, the gap is decreased. Therefore, the peaks of the specific heat contributed from β and γ spectra move to lower temperatures with the height decreased while those from α and λ spectra shift to higher temperatures with the height declined, both of which compose the observed shoulder and double peaks in the specific heat. As the spectra β and γ shift slowly with J_F but rapidly with J_{AF_2}, the specific heat exhibits a shoulder with increasing J_F but double peaks with increasing J_{AF_2} at low temperature. The three peaks in the specific heat that cannot be reproduced in the mean-field theory may result from the interactions of the quasiparticles, which might induce excitations between $\alpha(\lambda)$ and $\beta(\gamma)$. It is expected that the energies of the induced excitations are enhanced with increasing J_F, yielding the observed shift of the novel peak from the low to high temperatures in Fig. 2(b).

C. Thermodynamics in magnetic fields

At zero temperature, the spectra α and β are fully occupied while γ and λ spectra are empty in the absence of magnetic field. Thus, the excitations at finite temperature are of the hole (α and β) and fermion (γ and λ) types, respectively. In a magnetic field, the energies of the spectra decrease, yielding the excitations with minus energies to become hole excitations at finite temperature. In this subsection, some typical thermodynamic behaviors could be explained by the combination of the hole and fermion excitations.

When $h_{c_1}<h<h_{c_2}$ and $h_{c_3}<h<h_s$, the minimum and maximum of $m(T)$ at low temperature are observed in the

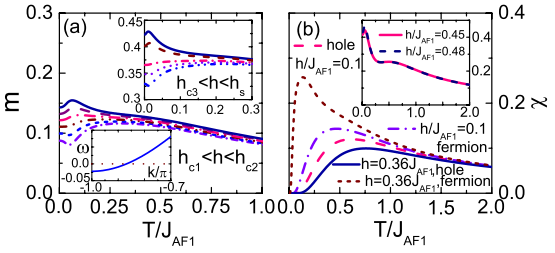

FIG. 10. (Color online) Mean-field results in different magnetic fields for (a) magnetization $m(T)$ at low temperatures in the gapless regime and (b) susceptibility contributed from the fermion and hole excitations. The lower inset of (a) depicts the dispersion in the vicinity of the lower critical field.

mean-field results, and the crossover temperatures in the gapless regime are lower than those in the LL, as shown in Fig. 10(a). As the magnetization is proportional to the total number of the fermions, the minimum and maximum indicate that the hole and fermion excitations dominate at low temperature, respectively. In the vicinity of the lower critical field $h_{c_1}(h_{c_3})$, the fermion spectrum $\gamma(\lambda)$ crosses the Fermi level slightly, as shown in the lower inset of Fig. 10(a), making the excitations with minus energies become hole type. Thus, the low-temperature behavior of $m(T)$ is determined by the competitions of the fermion and hole excitations near the Fermi level. Due to the dispersion relation, the density of states $D(\omega)$ of the holes is larger than that of the fermions near the Fermi level, yielding more holes excited and thus the decrease in m at low temperature. After the few holes are occupied, the fermion excitations dominate and, thus, a minimum of m emerges. The analogous arguments for the maximum near the upper critical field $h_{c_2}(h_s)$ also apply. The lower crossover temperature in the gapless regime is attributed to the larger values of the gradient of the Fermi velocity with respect to the field $\partial v_F/\partial h$ of the spectrum λ near the Fermi level, which diminishes the difference in the density of states in the vicinity of the Fermi level.

Different from the magnetization, the fermion and hole excitations have equivalent contributions to the susceptibility. However, with increasing the field, the fermion excitations move close to the Fermi surface while the holes move away. Thus, the peak of the susceptibility from the excited fermions shifts to lower temperatures with the height enhanced while that from the excited holes exhibits opposite behaviors, as shown in Fig. 10(b). All the observed behaviors of the susceptibility in the gapped spin liquid and plateau phases can be understood on the basis of the above analyses, as mentioned in Sec. III.

Now let us discuss briefly the specific heat. The specific heat can be divided into those from the fermion and hole excitations, which are denoted as C_f and C_h, respectively. It is found that C_f and C_h behave rather differently with the field and C_h contributes essentially to the observed characteristic features, which are not shown here for brevity. For example, when $h<h_{c_1}$, the gaps of the hole excitations α and β are enhanced with increasing the field, making the peaks of C_h move to higher temperatures with the amplitude decreased. As h approaches h_{c_1}, a low-temperature peak in C_h emerges, yielding the shoulder in the specific heat. In other phases, similar analyses are also applicable.

As discussed above, the spinless fermion mapping can be used to explain both the ground-state and thermodynamic properties in a wide range of the parameters. The fermion and hole excitations provide a simple way to understand the complex thermodynamic behaviors of the system.

V. SUMMARY AND DISCUSSION

The thermodynamic properties of the spin $S=1/2$ tetrameric HAFC with alternating couplings AF_1-AF_2-AF_1-F have been studied by means of the TMRG method and JW transformation. In the absence of magnetic field, the thermodynamic behaviors are determined by the gapped low-lying

excitations. The specific heat can have single peak, double peaks, and three peaks for different couplings. The shoulder and double peaks in the specific heat are attributed to the decreased energies of the gapped excitations. The novel intermediate peak in the specific heat results from the increase in J_F after the double peaks have been induced by large J_{AF_2}. With further increase in J_F, the novel peak shifts to higher temperatures and finally merges into the high-temperature peak. The susceptibility is found to have a peak that shifts to lower temperatures with the amplitude enhanced with increasing J_F or J_{AF_2}.

A phase diagram in the temperature-field plane for $J_{AF_1}=J_{AF_2}=J_F$ is obtained by analyzing the crossover behaviors of the various phases at finite temperature. The system is unveiled to contain the gapped spin liquid, LL, magnetization plateau, gapless, spin polarized, and classical phases.

In the LL and gapless regimes, the magnetization curve exhibits a minimum or maximum at low temperature, representing a nonsingular crossover. The linear field dependence of the crossover temperature in the LL with the same ratio as that in the $S=1$ Haldane chain indicates that the crossovers in the two systems belong to the same class, which implies that the Haldane-type phase of this tetrameric HAFC has an analogous low-lying dispersion relation to that in the $S=1$ Haldane chain. In the plateau state, as a crossing of a fermion and a hole spectra at h_m, the temperature dependence of the magnetization behaves differently below and above the field.

When $h<h_{c_1}$, the susceptibility has double peaks with increasing the field. In the plateau state, the susceptibility has a single peak, and owing to the crossing of the spectra, the peak moves to higher temperatures when $h<h_m$, and to lower temperatures when $h>h_m$ with increasing the field. In the LL and gapless regimes, χ is finite as $T\rightarrow 0$. The susceptibility in any fields coincides when $T>\Delta$ due to the thermal fluctuations.

In the gapped spin liquid, the specific heat has a shoulder as the field approaches the critical field h_{c_1}. In the LL, the specific heat as a function of temperature behaves linearly at low temperature and the shoulder is smoother down gradually by increasing the field. In the plateau, owing to the crossing of spectra, the peak of the specific heat moves to lower temperatures when $h<h_m$, and to higher temperatures when $h>h_m$ with increasing the field. As the field approaches h_{c_3}, a small peak emerges at low temperatures. In the gapless phase, with increased field $h-h_{c_3}$, the low-temperature peak moves to lower temperature with the amplitude decreased.

By means of the JW transformation and mean-field approximation, the low-lying excitations and thermodynamic properties of the system are studied to understand the TMRG results. It is unveiled that the system has four excitation spectra with a gap, which may account for the magnetization process at zero temperature. At finite temperature, it is found that the thermodynamic behaviors are determined by the combination of the fermion and hole excitations. The complex thermodynamic behaviors in the TMRG results can be understood well within the free fermion mapping. Finally, we would like to add that the observations presented in this paper for this spin-$\frac{1}{2}$ tetrameric HAFC could be expected to test experimentally in future.

ACKNOWLEDGMENTS

We are grateful to Bo Gu, Wei Li, Yang Zhao, and Guang-Qiang Zhong for useful discussions. This work is supported in part by the National Science Fund for Distinguished Young Scholars of China under Grant No. 10625419, the MOST of China under Grant No. 2006CB601102, and the Chinese Academy of Sciences.

*Corresponding author; gsu@gucas.ac.cn

[1] A. Brooks Harris, Phys. Rev. B **7**, 3166 (1973).
[2] G. S. Uhrig and H. J. Schulz, Phys. Rev. B **54**, R9624 (1996).
[3] T. Barnes, J. Riera, and D. A. Tennant, Phys. Rev. B **59**, 11384 (1999).
[4] A. W. Garrett, S. E. Nagler, D. A. Tennant, B. C. Sales, and T. Barnes, Phys. Rev. Lett. **79**, 745 (1997); B. Lake, R. A. Cowley, and D. A. Tennant, J. Phys.: Condens. Matter **9**, 10951 (1997); Guangyong Xu, C. Broholm, Daniel H. Reich, and M. A. Adams, Phys. Rev. Lett. **84**, 4465 (2000); M. B. Stone, W. Tian, M. D. Lumsden, G. E. Granroth, D. Mandrus, J.-H. Chung, N. Harrison, and S. E. Nagler, *ibid.* **99**, 087204 (2007).
[5] K. Hida, Phys. Rev. B **45**, 2207 (1992); J. Phys. Soc. Jpn. **63**, 2514 (1994).
[6] S. Watanabe and H. Yokoyama, J. Phys. Soc. Jpn. **68**, 2073 (1999).
[7] W. Zheng, C. J. Hamer, and R. R. P. Singh, Phys. Rev. B **74**, 172407 (2006).
[8] J. C. Livermore, R. D. Willett, R. M. Gaura, and C. P. Landee, Inorg. Chem. **21**, 1403 (1982); Y. Ajiro, T. Asano, T. Inami, H. Aruga-Katori, and T. Goto, J. Phys. Soc. Jpn. **63**, 859 (1994).
[9] M. A. M. Abu-Youssef, M. Drillon, A. Escuer, M. A. S. Goher, F. A. Mautner, and R. Vicente, Inorg. Chem. **39**, 5022 (2000).
[10] S. Martin, M. G. Barandika, L. Lezama, J. L. Pizarro, Z. E. Serna, J. I. R. de Larramendi, M. I. Arriortua, T. Rojo, and R. Cortés, Inorg. Chem. **40**, 4109 (2001).
[11] A. K. Ghosh, D. Ghoshal, E. Zangrando, J. Ribas, and N. R. Chaudhuri, Inorg. Chem. **44**, 1786 (2005).
[12] K. Okamoto, Solid State Commun. **98**, 245 (1996); A. Kitazawa and K. Okamoto, J. Phys.: Condens. Matter **11**, 9765 (1999).
[13] A. Honecker, Phys. Rev. B **59**, 6790 (1999).
[14] W. Chen, K. Hida, and B. C. Sanctuary, J. Phys. Soc. Jpn. **69**, 3414 (2000); Phys. Rev. B **63**, 134427 (2001).
[15] B. Gu, G. Su, and S. Gao, J. Phys.: Condens. Matter **17**, 6081 (2005); Phys. Rev. B **73**, 134427 (2006); B. Gu and G. Su, Phys. Rev. Lett. **97**, 089701 (2006); Phys. Rev. B **75**, 174437 (2007).
[16] S. S. Gong, B. Gu, and G. Su, Phys. Lett. A **372**, 2322 (2008).
[17] M. Oshikawa, M. Yamanaka, and I. Affleck, Phys. Rev. Lett. **78**, 1984 (1997).
[18] A. Escuer, R. Vicente, M. S. El Fallah, M. A. S. Goher, and F. A. Mautner, Inorg. Chem. **37**, 4466 (1998).

[19] M. Hagiwara, Y. Narumi, K. Minami, K. Kindo, H. Kitazawa, H. Suzuki, N. Tsujii, and H. Abe, J. Phys. Soc. Jpn. **72**, 943 (2003).
[20] S. Yamamoto, Phys. Rev. B **69**, 064426 (2004).
[21] T. Nakanishi and S. Yamamoto, Phys. Rev. B **65**, 214418 (2002).
[22] H. T. Lu, Y. H. Su, L. Q. Sun, J. Chang, C. S. Liu, H. G. Luo, and T. Xiang, Phys. Rev. B **71**, 144426 (2005).
[23] S. S. Gong and G. Su, Phys. Rev. B **78**, 104416 (2008).
[24] F. D. M. Haldane, Phys. Rev. Lett. **50**, 1153 (1983); Phys. Lett. **93A**, 464 (1983).
[25] I. Affleck, T. Kennedy, E. H. Lieb, and H. Tasaki, Phys. Rev. Lett. **59**, 799 (1987); Commun. Math. Phys. **115**, 477 (1988).
[26] H. Watanabe, K. Nomura, and S. Takada, J. Phys. Soc. Jpn. **62**, 2845 (1993).
[27] T. Barnes and J. Riera, Phys. Rev. B **50**, 6817 (1994).
[28] M. P. M. den Nijs and K. Rommelse, Phys. Rev. B **40**, 4709 (1989).
[29] T. Kennedy and H. Tasaki, Phys. Rev. B **45**, 304 (1992).
[30] S. Sachdev, *Quantum Phase Transitions* (Cambridge University Press, Cambridge, England, 1999).
[31] R. J. Bursill, T. Xiang, and G. A. Gehring, J. Phys.: Condens. Matter **8**, L583 (1996).
[32] X. Wang and T. Xiang, Phys. Rev. B **56**, 5061 (1997).
[33] T. Xiang and X. Wang, in *Density-Matrix Renormalization: A New Numerical Method in Physics*, edited by I. Peschel, X. Wang, M. Kaulke, and K. Hallberg (Springer, New York, 1999), pp. 149–172.
[34] X. Wang and Lu Yu, Phys. Rev. Lett. **84**, 5399 (2000).
[35] R. Chitra and T. Giamarchi, Phys. Rev. B **55**, 5816 (1997).
[36] Y. Maeda, C. Hotta, and M. Oshikawa, Phys. Rev. Lett. **99**, 057205 (2007).
[37] I. Affleck, Phys. Rev. B **41**, 6697 (1990); **43**, 3215 (1991).
[38] H. J. Schulz, Phys. Rev. B **22**, 5274 (1980).
[39] E. H. Lieb and W. Liniger, Phys. Rev. **130**, 1605 (1963).
[40] S. Yamamoto and S. Miyashita, Phys. Rev. B **48**, 9528 (1993).
[41] S. Sachdev, Phys. Rev. B **55**, 142 (1997).
[42] P. Jordan and E. Wigner, Z. Phys. **47**, 631 (1928).